

Photorefractive properties of undoped, cerium-doped, and iron-doped single-crystal $\text{Sr}_{0.6}\text{Ba}_{0.4}\text{Nb}_2\text{O}_6$

George A. Rakuljic
Amnon Yariv

California Institute of Technology
Department of Applied Physics
Pasadena, California 91125

Ratnakar Neurgaonkar

Rockwell International Corporation
Science Center
Thousand Oaks, California 91360

Abstract. We present the results of our theoretical and experimental studies of the photorefractive effect in single-crystal SBN:60, SBN:Ce, and SBN:Fe. The two-beam coupling coefficients, response times, and absorption coefficients of these materials are given.

Subject terms: photorefractive materials; nonlinear optical materials; optical phase conjugation; image processing; optical signal processing.

Optical Engineering 25(11), 1212-1216 (November 1986).

CONTENTS

1. Introduction
2. Material properties
3. Photorefractive properties
4. Summary of results
5. Conclusion
6. Acknowledgments
7. References

1. INTRODUCTION

A given photorefractive material is considered useful for optical processing applications such as phase conjugate optics if it possesses three important features: low response time, large coupling coefficient, and high optical quality. Speed is necessary if the crystal is to be used in real-time applications, and a large photorefractive coupling coefficient is required for the construction of efficient devices. Regardless of its speed and gain, however, a crystal with poor optical quality is of little practical importance. Although a material is yet to be found that completely satisfies all three requirements, here we show how well SBN:60 approximates them.

2. MATERIAL PROPERTIES

Strontium barium niobate (SBN) belongs to a class of tungsten bronze ferroelectrics that are pulled from a solid solution of alkaline earth niobates. The crystal is transparent and can be grown with a variety of ferroelectric and electro-optic properties, depending on the specific cation ratios introduced into the structure. In SBN the unit cell contains 10 NbO_6 octahedra, with only five alkaline earth cations to fill 10 interstitial sites.¹⁻³ The structure is thus incompletely filled, which permits the addition of a wide range of dopants into the host crystal. The general formula for SBN is $\text{Sr}_x\text{Ba}_{1-x}\text{Nb}_2\text{O}_6$, so SBN:60 represents $\text{Sr}_{0.6}\text{Ba}_{0.4}\text{Nb}_2\text{O}_6$.

Paper 2182 received Aug. 13, 1985; revised manuscript received July 16, 1986; accepted for publication July 18, 1986; received by Managing Editor July 29, 1986. This paper is a revision of Paper 567-04 which was presented at the SPIE conference on Advances in Materials for Active Optics, Aug. 22-23, 1985, San Diego, Calif. The paper presented there appears (unrefereed) in SPIE Proceedings Vol. 567.
© 1986 Society of Photo-Optical Instrumentation Engineers.

The point group symmetry of SBN is 4 mm, which implies that its electro-optic tensor is nonzero. The dominant electro-optic coefficient is r_{33} , which ranges from 100 pm/V in SBN:25 to 1400 pm/V in SBN:75. In order to realize the large values of electro-optic coefficients in SBN crystals, they must, in practice, be poled by first being heated to above their Curie points and then being cooled to room temperature with an applied dc electric field of 5 to 8 kV/cm.

3. PHOTOREFRACTIVE PROPERTIES

Single crystals of SBN:60, SBN:Ce ($\text{Sr}_{0.6}\text{Ba}_{0.4}\text{Nb}_2\text{O}_6:\text{Ce}$), and SBN:Fe ($\text{Sr}_{0.6}\text{Ba}_{0.4}\text{Nb}_2\text{O}_6:\text{Fe}$) grown at Rockwell International Corporation were studied using the two-wave mixing experiment shown in Fig. 1 to determine their effectiveness as photorefractive media. In Fig. 1 beams 1 and 2 are plane waves that intersect in the crystal and thus form an intensity interference pattern. Charge is excited by this periodic intensity distribution into the conduction band, where it migrates under the influence of diffusion and drift in the internal electric field and then preferentially recombines with traps in regions of low irradiance. A periodic space charge is thus created that modulates the refractive index by means of the electro-optic effect. This index grating, being out of phase with the intensity distribution, introduces an asymmetry that allows one beam to be amplified by constructive interference with light scattered by the grating while the other beam is attenuated by destructive interference with diffracted light. This process is shown graphically in Fig. 2. Although it is implicitly assumed here that the only photocarriers in SBN:60 are electrons, it is acknowledged that holes may also participate in the photorefractive effect. Experiments are currently under way to resolve this issue.

Mathematically, this two-beam coupling may be described in the steady state as follows:

$$\frac{dI_1}{d\xi} = -\Gamma \frac{I_1 I_2}{I_1 + I_2} - \alpha I_1, \quad (1)$$

$$\frac{dI_2}{d\xi} = \Gamma \frac{I_1 I_2}{I_1 + I_2} - \alpha I_2, \quad (2)$$

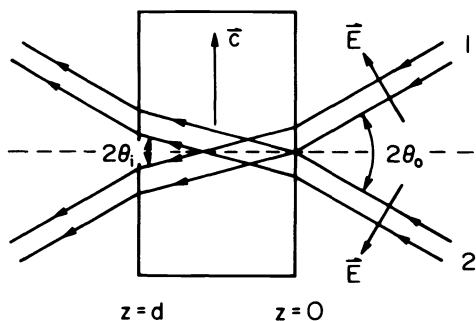


Fig. 1. Experimental setup for two-beam coupling experiments.

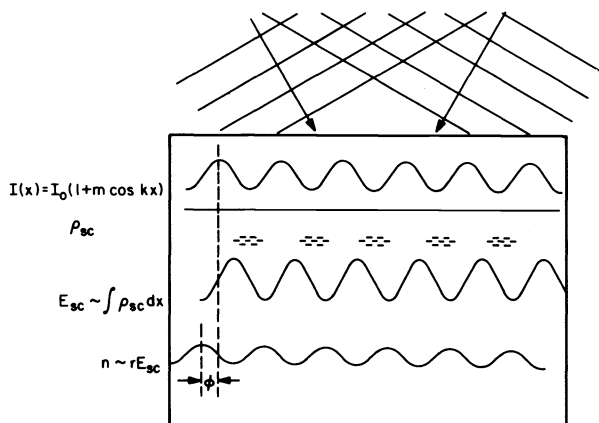


Fig. 2. The photorefractive mechanism. Two laser beams intersect, forming an interference pattern. Charge is excited where the intensity is large and migrates to regions of low intensity. The electric field associated with the resultant space charge operates through the electro-optic coefficients to produce a refractive index grating.

where I_1 and I_2 are the intensities of beams 1 and 2 inside the crystal, respectively, Γ is the two-beam coupling coefficient, α is the absorption coefficient, and $\xi = z/\cos\theta_i$, where $0 \leq \xi \leq \ell = d/\cos\theta_i$. The transient behavior is approximated by

$$I_i(\xi; t) = (1 - e^{-t/\tau})I_i(\xi; t \rightarrow \infty) + e^{-t/\tau}I_i(\xi; t = 0),$$

$$i = 1, 2, \quad (3)$$

where τ is a characteristic time constant and

$$I_i(\xi; t \rightarrow \infty) = I_i(\xi). \quad (4)$$

The solutions of the above coupled-wave equations are

$$I_1(\ell) = \frac{[I_1(0) + I_2(0)]e^{-\alpha\ell}}{1 + \frac{I_2(0)}{I_1(0)} e^{\Gamma\ell}}, \quad (5)$$

$$I_2(\ell) = \frac{[I_1(0) + I_2(0)]e^{-\alpha\ell}}{1 + \frac{I_1(0)}{I_2(0)} e^{-\Gamma\ell}}. \quad (6)$$

By measurement of the four intensities $I_1(0)$, $I_2(0)$, $I_1(\ell)$, and $I_2(\ell)$, both in the steady state and as a function of time, the two-beam coupling coefficient Γ and the response time τ can

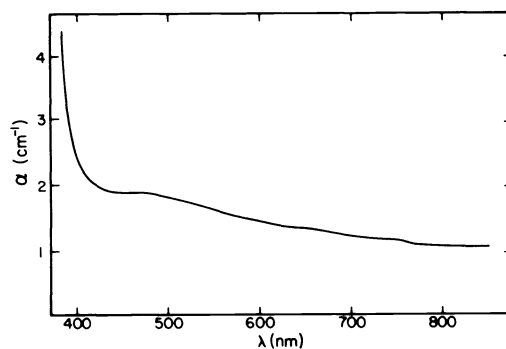


Fig. 3. Absorption spectrum of SBN:Ce.

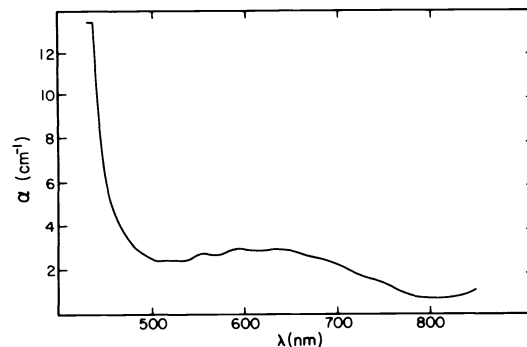


Fig. 4. Absorption spectrum of SBN:Fe.

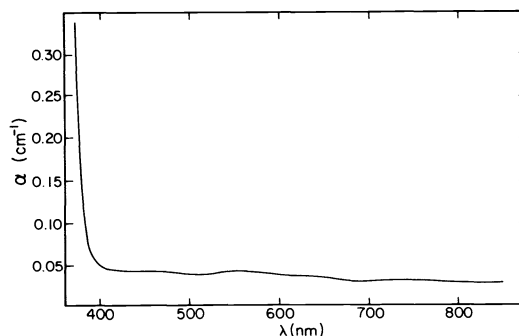


Fig. 5. Absorption spectrum of SBN:60.

be obtained from the above equations. It is important to note that although the above description of the transient behavior is not strictly correct,⁴ it does indeed approximate the temporal response of the two-wave mixing process in SBN very well since the measured waveforms can be accurately described by simple exponentials.

Maximum coupling will result in crystals with large Γ but small α . However, α and Γ are not independent. In fact, since charge must be excited into a conduction band by the intensity interference pattern in order to start the photorefractive process, some absorption is necessary. This is precisely where the role of the dopant enters. If impurities are purposely introduced into the crystal, donor sites are created that become the absorption centers. It must be noted, however, that any absorption that does not contribute to the photorefractive mechanism is undesirable.

Figures 3 and 4 show the effect of cerium and iron impurities on the absorption spectrum of undoped SBN, which is given in Fig. 5. Several interesting observations can be made. First, the band edge shifts from 400 nm in SBN:60 to 430 nm in SBN:Ce and 500 nm in SBN:Fe. Second, although the

SBN:60 was not intentionally doped, deep-level impurities are evidenced by perturbations in the spectrum near 550 nm. Finally, the effects of Ce and Fe in SBN:60 are seen to be significantly different. While the spectrum of SBN:Ce is rather featureless, with a broad deep level centered at 480 nm, the spectrum of SBN:Fe displays a structured but broad absorption extending from 500 to 700 nm, with characteristic peaks at 550 nm and 590 nm. Future investigation of these lines will indicate whether or not they contribute to the photorefractive effect.

First principle calculations using the band transport model⁵ can be used to derive expressions for Γ and τ . Solutions to the photorefractive equations developed most fully by Kukhta-
rev⁶⁻⁸ show that Γ and τ can be represented functionally as

$$\Gamma = \Gamma(d_g, E_0, \lambda, T; r, N_D, N_A, \epsilon, n), \quad (7)$$

$$\tau = \tau(d_g, E_0, \lambda, T, I_0; s, \gamma_R, \mu, N_D, N_A, \epsilon), \quad (8)$$

where the experimentally controlled variables are

d_g = grating period

E_0 = applied field (normal to grating planes)

λ = wavelength of incident light

T = temperature

I_0 = total irradiance

and the material parameters are

r = effective electro-optic coefficient

s = photoionization cross section

γ_R = two-body recombination rate

μ = mobility

N_D = number of donors under dark conditions

N_A = number of traps under dark conditions

ϵ = static dielectric constant

n = background refractive index .

These equations were applied to cerium-doped SBN. Specifically, the sample contained 10^{18} to 10^{19} cm⁻³ cerium atoms, which resulted in an as-grown crystal with $\Gamma = 11$ cm⁻¹, $\tau = 0.10$ s, and $\alpha = 1.8$ cm⁻¹ at $I_0 = 1$ W/cm², $T = 298$ K, $\lambda = 0.5145$ μ m, $E_0 = 0$ V/cm, and $d_g = 5$ μ m.

Variations in Γ and τ about this "operating point" are shown in Figs. 6 through 13, along with the experimentally obtained values of the two-beam coupling coefficient and response times for SBN:60 and SBN:Ce. Data for SBN:Fe are not shown since striations in the crystal so affected the optical quality of the crystal that no reliable experimental values could be measured. Although the SBN:60 and SBN:Ce samples were striation free and displayed good optical quality, to date all of the SBN:Fe crystals, regardless of their Fe concentration, have been severely marked with striations. We believe that better control of the melt temperature will eliminate this problem.

With no applied field, Fig. 7 indicates that Γ should be greater than 1 cm⁻¹ for all practical values of d_g , while the application of an electric field of 2 kV/cm ought to increase the coupling coefficient to 35 cm⁻¹ at $d_g = 5$ μ m, as shown in Fig. 8. Such a large response would then make even very thin samples of SBN:Ce useful photorefractive media. However, in practice, these large values of Γ are not easily obtainable. As an electric field is applied to the crystal, induced stresses deform the material and the incident beams are distorted. Therefore, we conclude that the application of an electric field to the crystal to control its two-beam coupling coefficient is of

limited use.

Another way Γ can be modified was suggested in Ref. 9. By varying the trap density N_A with reduction and oxidation treatments, one should be able to control Γ , as shown in Fig. 9. Although the exact number density of traps is difficult to measure, we have indeed been able to change the two-beam coupling coefficient from less than 0.1 cm⁻¹ to 15 cm⁻¹ by heating the crystal in atmospheres with different oxygen partial pressures.

The predicted variation of response time with trap density, which is shown in Fig. 10, has yet to be observed in SBN:Ce. Although Γ decreases as expected when the crystal is heated in a reducing atmosphere, the time constant remains unchanged at a typical value of 100 ms at 1 W/cm² irradiance. This unexpected and currently unexplained result has complicated our effort to produce a cerium-doped SBN photorefractive crystal with 1 ms response time, since heat treatment was proposed as a method of achieving this goal.⁹ Therefore, other techniques may need to be invoked to obtain the desired speed of response.

Figures 11, 12, and 13 show how the response time τ is affected by changes in the mobility μ , the two-body recombination rate γ_R , and the photoionization cross section s , respectively. Since μ is predominantly an intrinsic quantity of the host crystal, little can be done to increase its value. However, s and γ_R are extrinsic parameters that can be varied by the selection of different dopants. If the dopant chosen has either a larger photoionization cross section or a smaller two-body recombination rate coefficient than is presently obtained with cerium, the resulting doped sample of SBN should have a shorter response time. The selection of such a dopant, unfortunately, is a nontrivial task.

Table I shows the results of an elemental analysis by nuclear activation of undoped and cerium-doped SBN. Since undoped SBN is photorefractive while containing only trace quantities of cerium, we must conclude that cerium is not the only photorefractive species for SBN. In fact, Table I indicates that there are significant amounts of Fe, Ni, Mo, and Ta impurities in the undoped SBN crystal, and Fe and Ni, for example, are known to be effective photorefractive centers in LiNbO₃.¹⁰ Although iron has already been used as a dopant for SBN, the resulting crystals were optically imperfect. Therefore, we suggest that not only should the study of iron- and cerium-doped SBN continue, but crystals doped with other impurities, which may prove to have better values of γ_R and s , should also be investigated.

4. SUMMARY OF RESULTS

A major goal of our work has been the growth of high optical quality photorefractive SBN crystals. This was accomplished in part by growing striation-free SBN:60 and SBN:Ce. In fact, optically excellent crystals of SBN:60 and SBN:Ce can now be had as cubes approaching 1 cm on a side. SBN:Fe, unfortunately, has yet to be grown without striations. As was indicated earlier, better control of the melt temperature may be necessary to eliminate this problem.

Large two-beam coupling was observed in both SBN:60 and SBN:Ce. Values of Γ ranged from 2 cm⁻¹ in SBN:60 to greater than 10 cm⁻¹ in SBN:Ce. Such response was large enough to permit the use of these crystals in the construction of the ring¹¹ and semilinear¹² passive phase conjugate mirrors, for example. It was also found that oxidation and reduction techniques served as effective methods for varying the value of

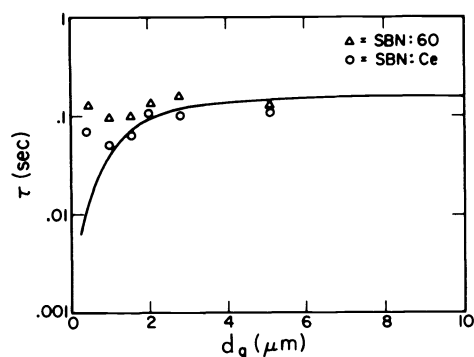


Fig. 6. Response time versus grating period at $I_0 = 1 \text{ W/cm}^2$ for $E_0 = 0 \text{ V/cm}$.

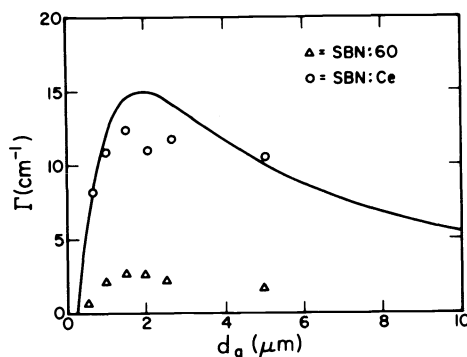


Fig. 7. Coupling coefficient versus grating period for $E_0 = 0 \text{ V/cm}$.

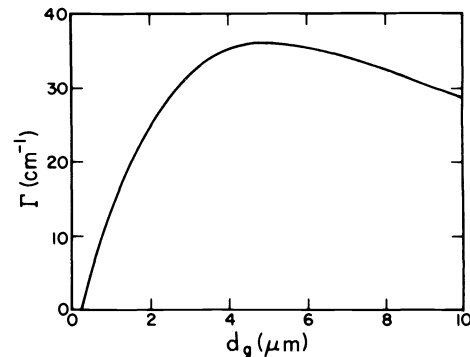


Fig. 8. Coupling coefficient versus grating period for $E_0 = 2 \text{ kV/cm}$.

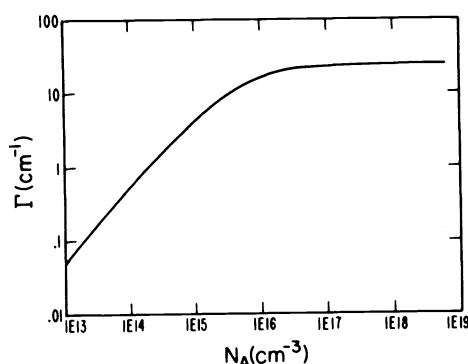


Fig. 9. Coupling coefficient versus trap density for $E_0 = 0 \text{ V/cm}$ and $d_g = 5 \text{ micrometers}$.

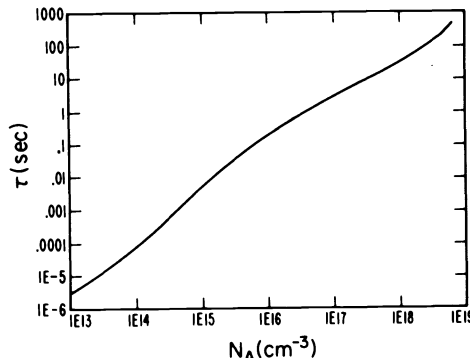


Fig. 10. Response time versus trap density at $I_0 = 1 \text{ W/cm}^2$, assuming $\mu = 0.1 \text{ cm}^2 \cdot \text{V}^{-1} \cdot \text{s}^{-1}$, $\gamma_R = 5 \times 10^{-8} \text{ cm}^3/\text{s}$, $s = 1.6 \times 10^{-19} \text{ cm}^2$, $N_D = 10^{19} \text{ cm}^{-3}$, and $d_g = 5 \text{ micrometers}$.

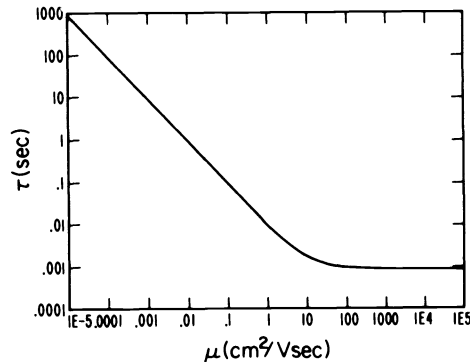


Fig. 11. Response time versus mobility at $I_0 = 1 \text{ W/cm}^2$, assuming $N_A = 10^{16} \text{ cm}^{-3}$, $\gamma_R = 5 \times 10^{-8} \text{ cm}^3/\text{s}$, $s = 1.6 \times 10^{-19} \text{ cm}^2$, $N_D = 10^{19} \text{ cm}^{-3}$, and $d_g = 5 \text{ micrometers}$.

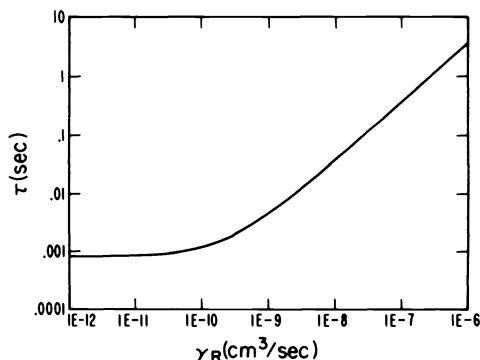


Fig. 12. Response time versus two-body recombination rate coefficient at $I_0 = 1 \text{ W/cm}^2$, assuming $N_A = 10^{16} \text{ cm}^{-3}$, $\mu = 0.1 \text{ cm}^2 \cdot \text{V}^{-1} \cdot \text{s}^{-1}$, $s = 1.6 \times 10^{-19} \text{ cm}^2$, $N_D = 10^{19} \text{ cm}^{-3}$, and $d_g = 5 \text{ micrometers}$.

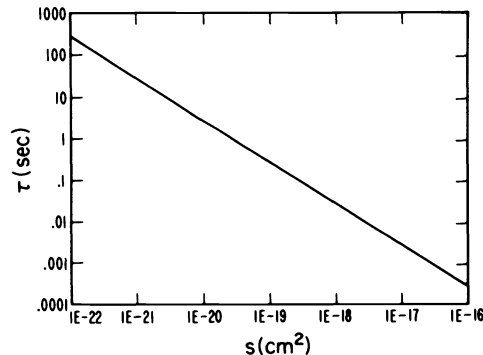


Fig. 13. Response time versus photoionization cross section at $I_0 = 1 \text{ W/cm}^2$, assuming $N_A = 10^{16} \text{ cm}^{-3}$, $\mu = 0.1 \text{ cm}^2 \cdot \text{V}^{-1} \cdot \text{s}^{-1}$, $\gamma_R = 5 \times 10^{-8} \text{ cm}^3/\text{s}$, $N_D = 10^{19} \text{ cm}^{-3}$, and $d_g = 5 \text{ micrometers}$.

Γ in these crystals. However, the application of an external electric field to the crystals tended to degrade their optical quality rather than improve the value of their coupling coefficients.

The response times of the SBN crystals we tested averaged about 100 ms for an incident irradiance of 1 W/cm^2 . In general, SBN:Ce responded quicker than SBN:60, with times approaching 50 ms at 1 W/cm^2 . Since the two-beam coupling coefficient of SBN:Ce is so large, the time required to reach a given diffraction efficiency with SBN:Ce will be much shorter than that needed with SBN:60. Although the response time of SBN:Fe has yet to be reliably determined, we believe that its speed will not differ significantly from that of the other two crystals.

5. CONCLUSIONS

High optical quality undoped and doped single-crystal SBN:60 has been grown and proved to be photorefractive. This effect was quantified by measuring the coupling coefficients and response times of several samples using the method of two-wave mixing. The results of this work indicate that the introduction of dopants into SBN:60 produces crystals with an even greater photorefractive effect than that of undoped SBN:60.

6. ACKNOWLEDGMENTS

This research was supported by grants from Rockwell International Corporation, the U.S. Air Force Office of Scientific Research, and the U.S. Army Research Office.

Elements & Units	SBN:60	SBN:Ce
U PPM	< 0.1	< 0.1
TH PPM	< 0.3	< 0.2
NA PPM	30.0	<30.0
SC PPM	0.04	0.04
CR PPM	< 5.0	< 5.0
FE %	0.029	0.014
CO PPM	0.3	0.3
NI PPM	50.0	50.0
ZN PPM	7.0	5.0
AS PPM	< 1.0	< 1.0
SE PPM	< 5.0	< 5.0
BR PPM	< 0.5	< 0.5
MO PPM	11.0	4.0
SB PPM	0.5	0.5
CS PPM	< 0.2	< 0.2
BA PPM	160000.0	150000.0
LA PPM	0.2	1.0
HF PPM	< 0.2	< 0.2
TA PPM	12.0	13.0
W PPM	< 3.0	1.0
AU PPB	< 5.0	5.0
CE PPM	< 1.0	47.0
ND PPM	Interfer	Interfer
SM PPM	0.01	0.32
EU PPM	0.07	0.10
TB PPM	< 0.1	< 0.1
YB PPM	< 0.05	0.05
LU PPM	< 0.01	< 0.01
SR PPM	148000.0	135000.0
RB PPM	< 5.0	< 5.0

1. P. B. Jamieson, S. C. Abrahams, and J. L. Bernstein, "Ferroelectric tungsten bronze-type crystal structures. I. Barium strontium niobate $\text{Ba}_{0.27}\text{Sr}_{0.73}\text{Nb}_2\text{O}_{7.78}$," J. Chem. Phys. 48, 5048 (1968).
2. P. B. Jamieson, S. C. Abrahams, and J. L. Bernstein, "Ferroelectric tungsten bronze-type crystal structures. II. Barium sodium niobate $\text{Ba}_{(4+x)}\text{Na}_{(2-2x)}\text{Nb}_{10}\text{O}_{30}$," J. Chem. Phys. 50, 4352 (1969).
3. S. C. Abrahams, P. B. Jamieson, and J. L. Bernstein, "Ferroelectric tungsten bronze-type crystal structures. III. Potassium lithium niobate $\text{K}_{(6-x-y)}\text{Li}_{(4+x)}\text{Nb}_{(10+y)}\text{O}_{30}$," J. Chem. Phys. 54, 2355 (1971).
4. J. M. Heaton and L. Solymar, "Transient energy transfer during hologram formation in photorefractive crystals," Opt. Acta 32(4), 397 (1985).
5. G. C. Valley and M. B. Klein, "Optimal properties of photorefractive materials for optical data processing," Opt. Eng. 22(6), 704-711 (1983).
6. N. V. Kukhtarev, V. B. Markov, and S. G. Odulov, "Transient energy transfer during hologram formation in LiNbO_3 in external electric field," Opt. Commun. 23, 338 (1977).
7. N. V. Kukhtarev, V. B. Markov, S. G. Odulov, M. S. Soskin, and V. L. Vinetski, "Holographic storage in electrooptic crystals. I. Steady state," Ferroelectrics 22, 949 (1979).
8. N. V. Kukhtarev, "Kinetics of hologram recording and erasure in electrooptic crystals," Sov. Tech. Phys. Lett. 2, 438 (1976).
9. G. A. Rakuljic, A. Yariv, and R. R. Neurgaonkar, "Photorefractive properties of ferroelectric BaTiO_3 and $\text{SBN}:60$," in *Nonlinear Optics and Applications*, P. Yeh, ed., Proc. SPIE 613, 110-118 (1986).
10. W. Phillips, J. J. Amodel, and D. L. Staebler, "Optical and holographic storage properties of transition metal doped lithium niobate," RCA Rev. 33, 94 (1972).
11. M. Cronin-Golomb, B. Fischer, J. O. White, and A. Yariv, "Passive phase conjugate mirror based on self-induced oscillation in an optical ring cavity," Appl. Phys. Lett. 42, 919 (1983).
12. M. Cronin-Golomb, B. Fischer, J. O. White, and A. Yariv, "Passive (self-pumped) phase conjugate mirror: theoretical and experimental investigation," Appl. Phys. Lett. 41, 689 (1982).



Professor Yariv has published widely in the laser and optics fields (some 300 papers) and has written a number of basic texts in quantum electronics, optics, and quantum mechanics. He is an associate editor of *Optics Communications* and was previously associate editor of the *Journal of Quantum Electronics* and the *Journal of Applied Physics*. He is a member of the American Physical Society, Phi Beta Kappa, the American Academy of Arts and Sciences, and the National Academy of Engineering and a Fellow of the IEEE and OSA. He received the 1980 Quantum Electronics Award of the IEEE, the 1985 University of Pennsylvania Pender Award, and the 1986 OSA Ives Medal. He is a founder and chairman of the board of ORTEL Corp.



surface acoustic wave, millimeter wave, and piezoelectric transducers. He and a coworker have developed various growth techniques for ferroelectric crystals/films and recently successfully demonstrated the growth of optical-quality doped and undoped $\text{Sr}_{1-x}\text{Ba}_x\text{Nb}_2\text{O}_6$ and BSKNN single crystals using the Czochralski technique. Besides ferroelectric materials, Dr. Neurgaonkar has been interested in magnetics, luminescence, and laser crystal development work. He is a member of various professional societies, including the American Ceramic Society, the Electrochemical Society, and the American Association for Crystal Growth. He is the author or coauthor of more than 70 research publications.